

## The influence of scaffold microstructure on chondrogenic differentiation of mesenchymal stem cells

This content has been downloaded from IOPscience. Please scroll down to see the full text.

2014 Biomed. Mater. 9 035011

(<http://iopscience.iop.org/1748-605X/9/3/035011>)

View [the table of contents for this issue](#), or go to the [journal homepage](#) for more

Download details:

IP Address: 162.105.25.9

This content was downloaded on 03/08/2014 at 04:18

Please note that [terms and conditions apply](#).

# The influence of scaffold microstructure on chondrogenic differentiation of mesenchymal stem cells

Jingjing Zhang<sup>1</sup>, Yingnan Wu<sup>2</sup>, Tanushree Thote<sup>3</sup>, Eng Hin Lee<sup>2,4</sup>, Zigang Ge<sup>1,5,6,7</sup> and Zheng Yang<sup>4,7</sup>

<sup>1</sup> Department of Biomedical Engineering, College of Engineering, Peking University, Beijing 100871, People's Republic of China

<sup>2</sup> Department of Orthopaedic Surgery, Yong Loo Lin School of Medicine, National University of Singapore, Singapore

<sup>3</sup> Wallace H Coulter Department of Biomedical Engineering, Georgia Institute of Technology, Atlanta, GA 30332, USA

<sup>4</sup> Tissue Engineering Program, Life Sciences Institute, National University of Singapore, 27 Medical Drive, Singapore 117510, Singapore

<sup>5</sup> Center for Biomedical materials and Tissue Engineering, Academy for Advanced Interdisciplinary Studies, Peking University, Beijing 100871, People's Republic of China

<sup>6</sup> Arthritis Clinic and Research Center, Peking University People's Hospital, Beijing, People's Republic of China

E-mail: [zjj4785@163.com](mailto:zjj4785@163.com), [mbiwy@nus.edu.sg](mailto:mbiwy@nus.edu.sg), [tthote@gatech.edu](mailto:tthote@gatech.edu), [eng\\_hin\\_lee@nuhs.edu.sg](mailto:eng_hin_lee@nuhs.edu.sg), [gez@pku.edu.cn](mailto:gez@pku.edu.cn) and [lsiyz@nus.edu.sg](mailto:lsiyz@nus.edu.sg)

Received 14 November 2013, revised 2 April 2014

Accepted for publication 15 April 2014

Published 12 May 2014

## Abstract

Different forms of biomaterials, including microspheres, sponges, hydrogels and nanofibres have been broadly used in cartilage regeneration; however, effects of internal structures of biomaterials on chondrogenesis of mesenchymal stem cells (MSCs) remain largely unexplored. Here we investigated the effect of physical microenvironments of sponges and hydrogels on chondrogenic differentiation of MSCs. MSCs, cultured in these two scaffold systems, were induced with TGF- $\beta_3$  in chondrogenic differentiation medium and the chondrogenic differentiation was evaluated and compared after three weeks. MSCs in the sponges clustered with spindle morphologies, while they distributed homogeneously with round morphologies in the hydrogel. The MSCs proliferated faster in the sponge compared to that in the hydrogel. Significantly higher glycosaminoglycan and collagen II were found in the sponges but not in the hydrogels. The different tissue formation ability of MSCs in these two systems could be attributed to the different metabolic requirements and the cellular events prerequisite in the chondrogenic process of MSCs. It is reasonable to conclude that sponges with relatively active microenvironments that facilitate cell–cell contacts and cell–matrix interaction are optimal for early stage of chondrogenic differentiation.

Keywords: mesenchymal stem cells, chondrogenesis, hydrogel, sponge, tissue engineering

(Some figures may appear in colour only in the online journal)

---

<sup>7</sup> Authors to whom any correspondence should be addressed.

## 1. Introduction

Various forms of biomaterials, including sponges (Wu *et al* 2010, Yang *et al* 2012), hydrogels (Hao *et al* 2010), microspheres (Choi *et al* 2010) and nanofibres (Li *et al* 2006) have been designed, fabricated and used in cartilage regeneration. However, comparison of cell behaviour in different types of biomaterials remains elusive. Multiple parameters, including mechanical, physical, chemical and biological properties of biomaterials have effects on distribution, morphology, cytoskeletal organization and proliferation of the cells as well as matrix production and maturation (Ge *et al* 2012, Nuernberger *et al* 2011, Li *et al* 2006, Wang *et al* 2011). This complexity makes direct comparison of different types of biomaterials challenging. Our previous study has shown that physical properties and internal structures of biomaterials have significant effects on the phenotypes of chondrocytes and subsequent chondrogenesis, attributed to differences in cell attachment, cellular distribution and aggregation in the scaffold (Zhang *et al* 2013).

Mesenchymal stem cells (MSCs) are an alternative cell source for cartilage regeneration due to the ease of extraction from various sites of tissues, high proliferation capacity and ability to differentiate into chondrocytes (Caplan 2005, Qi *et al* 2012). Even though MSCs can be coaxed into chondrogenic differentiation indicated by the expressions of type II collagen and glycosaminoglycan (GAG), these induced-MSCs are inherently different from the articular chondrocytes in many aspects, such as their tendency to undergo hypertrophic development (Kang *et al* 2012, Saha *et al* 2010). Limited differentiation of MSCs-derived chondrocytes coupled with less ECM formation results in tissue with inferior biochemical and mechanical properties compared to that generated by chondrocytes (Qing *et al* 2011, Vinardell *et al* 2011). Compared to the low mitotic, terminally differentiated matured chondrocytes, MSCs are progenitor cells, having higher proliferation capacity and multi-potent ability to differentiate into several cell types. The spherical morphology of chondrocytes is closely related to their chondrogenic potential (Zanetti and Solursh 1984). MSCs, on the other hand, are fibroblastic cells *in vitro* and have to undergo a series of tightly orchestrated differentiation processes in which cell migration, proliferation and aggregation facilitated by cell–matrix and cell–cell interactions are essential (Goldring *et al* 2006). Morphologically, chondrogenic progenitor cells have their fibroblast-like shape transform into spherical morphology typical of chondrocytes and commence synthesis of cartilage-specific ECM molecules (Woods *et al* 2007).

Given the differences in the developmental status of chondrocytes and MSCs, it is possible that a scaffold system suitable for chondrocyte tissue formation might not meet the optimal requirements for chondrogenic differentiation of MSCs. Following up on our previous study examining effects of physical properties of the microenvironments on chondrocytes using chitosan-fabricated sponge and chitosan hydrogel (Zhang *et al* 2013), this study was set up to explore effects of these physical microenvironments on chondrogenic differentiation of MSCs. We evaluated the distribution,

morphology, proliferation and chondrogenic differentiation of MSCs in both chitosan sponges and chitosan hydrogel, with an aim to understand the effects of physical properties and 3D internal structures of these materials on chondrogenesis of MSCs.

## 2. Materials and methods

### 2.1. Fabrication of sponges and hydrogels of chitosan

Chitosan (poly( $\beta$ -(1-4-2-amino-2-deoxy-D-glucopyranose)) (degree of deacetylation 80–95%; viscosity 50–800 mPa s; pH 3.5, 69 047 460, Guoyao Chemical Reagents Limited, Beijing, China) was dissolved in 2 M acetic acid to obtain 3% chitosan solution. The solution was frozen at  $-80^{\circ}\text{C}$  and lyophilized, before being rehydrated and hardened with NaOH/ethanol mixture and lyophilized again. The sponges were sterilized with 75% ethanol and washed with PBS prior to use. The chitosan hydrogels were made by mixing filter-sterilized  $\beta$ -sodium glycerophosphate (GP, Sigma, 11.5% w/v, molecular weight 216.04) with 3% chitosan and 10% GP (Hoemann *et al* 2005). The resulting chitosan-GP solution was incubated at  $37^{\circ}\text{C}$  for 15–30 min to form a hydrogel.

### 2.2. Characterization of sponge and hydrogel

The morphology of the lyophilized sponge and dry hydrogel was observed by scanning electron microscopy (SEM; Quanta 200FEG, FEI, USA) with the accelerating voltage set at 15 kV. The microstructure of the sponge immersed in PBS and freshly made hydrogel was analysed by environmental scanning electron microscopy (ESEM, AMRAY-1910FE).

### 2.3. MSC cell culture

MSCs were harvested from bone marrow aspirates of pigs. The bone marrow cells were washing with HBSS (Invitrogen, Grand Island, NY) before incubating in DMEM (Invitrogen) containing 10% FBS (Invitrogen) at  $37^{\circ}\text{C}$  in 5%  $\text{CO}_2$  atmosphere. After 72 h, nonadherent cells were washed out. When 70%–80% confluence was reached, adherent cells were trypsinized and further expanded. A homogenous MSC population was obtained after 1–2 weeks of culture, and MSCs were used between passage 3 and 5.

### 2.4. Chondrogenic differentiation of MSCs

Chondrogenic differentiation media contained high glucose DMEM supplemented with  $10^{-7}$  M dexamethasone (Sigma, St Louis, MO),  $50\ \mu\text{g ml}^{-1}$  ascorbic acid, 1 mM sodium pyruvate (Sigma), 4 mM proline (Sigma), 1% ITS+ premix (BD Bioscience Inc., Franklin Lakes, NJ) and  $10\ \text{ng ml}^{-1}$  of TGF- $\beta_3$  (R&D Systems, Minneapolis, MN). The cell-scaffold constructs were incubated at  $37^{\circ}\text{C}$  in 5%  $\text{CO}_2$ .

Two cell densities of MSCs ( $4 \times 10^6$  and  $10 \times 10^6\ \text{cells ml}^{-1}$ ) were seeded onto both scaffolds. For the chitosan sponge, MSCs at the above concentration were seeded onto the blotted dry scaffolds, allowed to adhere for 2 h before being cultured in MSCs culture medium overnight.

For the chitosan hydrogel, the chitosan-GP solution mixed with cells was incubated for 30 min at 37 °C to form the hydrogel. Medium was then added, with changes of media several times to remove the acidity of the hydrogel until the pH of the media was equilibrated to neutrality. Chondrogenic differentiation was induced by culturing the samples in chondrogenic differentiation media the next day. All scaffolds were cultured in 24 well plates and culture medium was changed at three days' interval.

### 2.5. Distribution and morphology of MSCs

The cell-scaffold constructs were incubated with 2 µg ml<sup>-1</sup> fluorescein diacetate (FDA, F7378, Sigma) for 15 min and washed three times before being stained with 5 µg ml<sup>-1</sup> of propidium iodide (PI, P4170, Sigma) for 5 min. The constructs were observed with confocal laser scanning microscopy (CLSM, LSM510, Zeiss, Germany) at an excitation wavelength of 488 nm. For F-actin staining, the samples were fixed with 4% paraformaldehyde and MSCs were permeabilized in 0.1% Triton X-100, stained with rhodamine phalloidin (PHDR1, cytoskeleton) for 30 min, followed by nuclear counterstaining with 4',6-diamidino-2-phenylindole (DAPI, Sigma, USA) for 2 h.

### 2.6. Metabolism and proliferation of MSCs

Metabolism of MSCs was measured by MTT assays (3-(4,5-dimethyl-2-thiazolyl)-2,5-diphenyl-2-tetrazolium bromide (M 2128, Sigma)). MSCs with cell density at 4 × 10<sup>6</sup> ml<sup>-1</sup> and 10 × 10<sup>6</sup> ml<sup>-1</sup> were seeded onto the sponges (5 × 5 × 2 mm<sup>3</sup>) or mixed with 50 µL of hydrogel before 100 µL of culture medium was added. After culturing for 1, 3 and 7 days, the MTT solution was added and the cells were incubated for 3 h before the absorbance was detected at 570 nm. This experiment was repeated four times.

The DNA amount in constructs was quantified by PicoGreen<sup>®</sup> dsDNA. Cell lysates were incubated with equal volume of PicoGreen in TE solution (10 mM Tris-HCl, 1 mM EDTA, pH 7.5) for 2–5 min at room temperature in 96 well black plates, protected from light. A FLUOstar Optima fluorescent plate reader (BMG Labtech, Offenburg, Germany) was used to quantify the sample solution at 350 nm excitation and 445 nm emission. This experiment was replicated three times.

### 2.7. sGAG quantification

The samples were digested in 0.25% collagenase type II solution at 37 °C for 2 h. Next the cells and the digested solution were collected by centrifugation and stored at -20 °C until assays. Blyscan sulfated glycosaminoglycan (sGAG) assay kit (Biocolor Ltd, Newtownabbey, Ireland) was used to measure the amount of sGAG according to the manufacturer's protocol. The digested solution was mixed with Blyscan dye and agitated for 30 min. After removing the unbound dye by high speed centrifuge, the precipitate was centrifuged down and dissolved with dissociation reagents. The absorbance of the re-dissolved solution was measured with FLUOstar Optima

plate reader at an absorbance wavelength of 656 nm. Triplicate samples from each condition were analysed.

### 2.8. Histology and immunohistochemistry

The samples were fixed in a 4% paraformaldehyde buffer (pH 7.4), then dehydrated and embedded in paraffin before sectioning at 5 µm. For alcian blue staining, the tissue sections were incubated with 0.5% alcian blue (Sigma) in 0.1 M HCl and counterstained with nuclear fast red (Sigma). For immunohistochemistry staining, hydrogen peroxide was used to block endogenous peroxidase in the tissue sections before pepsin treatment. Monoclonal antibodies of collagen type II (Clone 6B3; Chemicon Inc.) with dilution of 1:500 and collagen type X (Clone X53, Quartett, Berlin, Germany) with dilution factor 1:25, were applied followed by biotinylated goat anti-mouse (Lab Vision Corporation, Fremont, CA) incubation. Streptavidin peroxidase was added and 3,3'-diaminobenzidine was used as the chromogenic agent. The samples were counterstained with Gill's hematoxylin.

### 2.9. Statistical analysis

Statistical significance between groups was analysed by SPSS17.0 (One-way ANOVA, LSD,  $P < 0.05$ ). Data are expressed as mean ± standard deviation with the significance level set at  $p < 0.05$ .

## 3. Results

### 3.1. The microstructure of sponge and hydrogel

As indicated by SEM, the dry sponge had a highly interconnected porous structure with pore size at about 100 µm (figure 1(a)), and the lyophilized hydrogel had comparable pore size but with lesser interconnectivity (figure 1(d)). The ESEM photographs showed that the pores of the wet sponge were much smaller than the dry one, but larger than the freshly made hydrogel. The fresh hydrogel had small pores (pore size less than 20 µm) (figures 1(e), (f)).

### 3.2. Cell proliferation, morphology and distribution in the scaffolds

Cell proliferation was analysed by MTT assay. The MSCs in sponges displayed higher proliferation (figure 2(a)). The cells proliferated significantly faster in the sponges ( $p < 0.01$ ), with an increase of nearly two-fold at day 7 when compared with day 1 both for low cell density and high cell density. Chitosan hydrogels with cell density of 10 × 10<sup>6</sup> ml<sup>-1</sup> (figure 2(c)) was apparently more than the hydrogels with 4 × 10<sup>6</sup> ml<sup>-1</sup> (figure 2(b)) at day 0. Significant difference between different cell densities in hydrogels was not only found at day 1, but also at day 3 and day 7. However, MSCs in the chitosan hydrogel had a slight increase (nearly 1.3 fold) from day 1 to day 3, but did not alter significantly from day 3 to day 7 in low nor high cell density. After seven days,

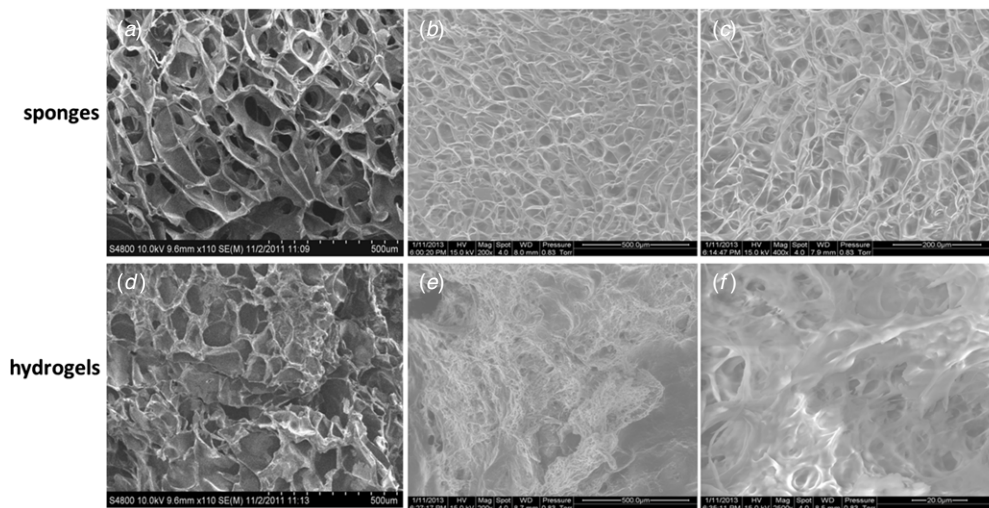


**Figure 1.** Morphology of sponge and hydrogel analysed by scanning electron micrographs (SEM) and environment scanning electron micrographs (ESEM). The morphology of dry sponge (a) and lyophilized hydrogel (d) by SEM. The structure of wet sponge (b) and (c) and fresh hydrogel (e) and (f) analysed by ESEM.

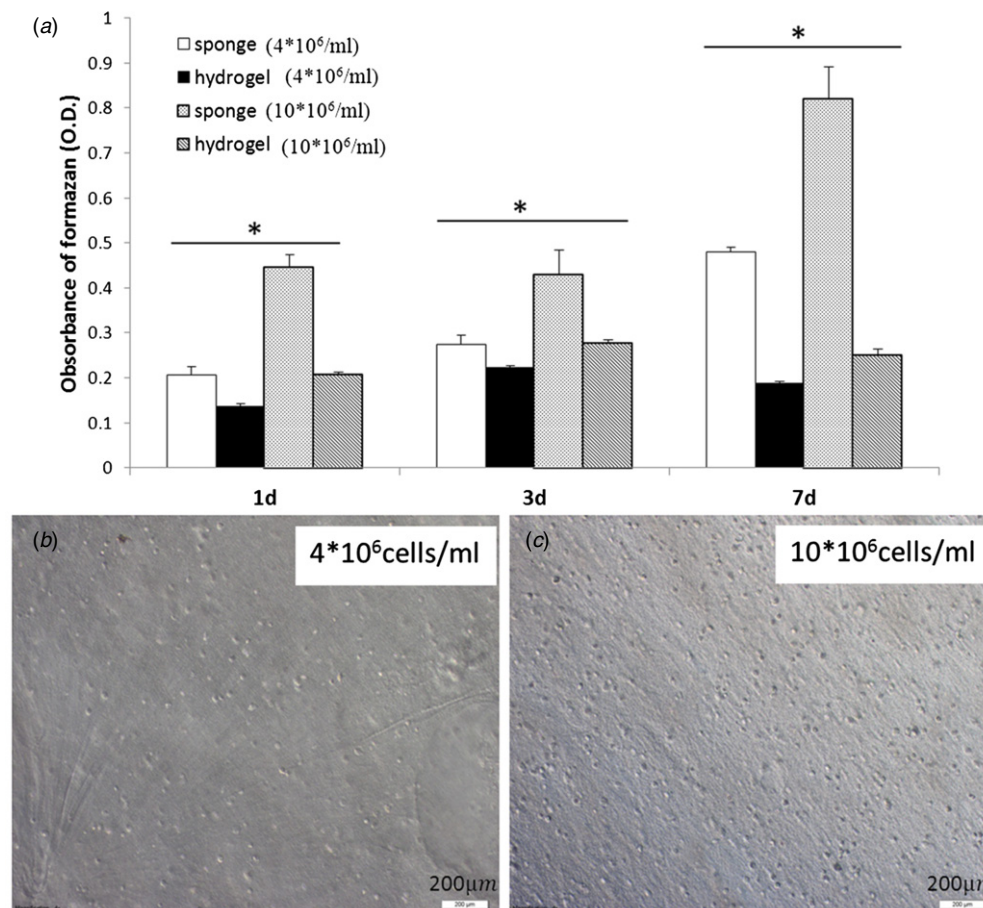


**Figure 2.** The proliferation of MSCs with cell density of  $4 \times 10^6/\text{ml}$  and  $10 \times 10^6/\text{ml}$  in chitosan sponges and chitosan hydrogels at 1, 3 and 7 days. (a) Cell proliferation was measured by MTT assay. (b) Representative image of MSCs with cell density  $4 \times 10^6 \text{ ml}^{-1}$  in chitosan hydrogels at day 0. (c) Microscopic photos of MSCs with cell density  $10 \times 10^6 \text{ ml}^{-1}$  in chitosan hydrogels at day 0. Each group compared with each other. Data expressed as mean  $\pm$  SD  $n = 4$ , One-Way ANOVA, LSD, \* represents  $P < 0.05$ . (The standard deviation was used to define the value of the error bars.) Scale bars: 200  $\mu\text{m}$ .

there was a 2.28-fold and 1.55-fold increase of absorbance in the sponge when compared with that of the hydrogel in low and high cell density, respectively.

Positive FDA staining in combination with weak PI staining, indicated that majority of MSCs in the sponges and in the hydrogel were viable cells. MSCs in the sponge at a

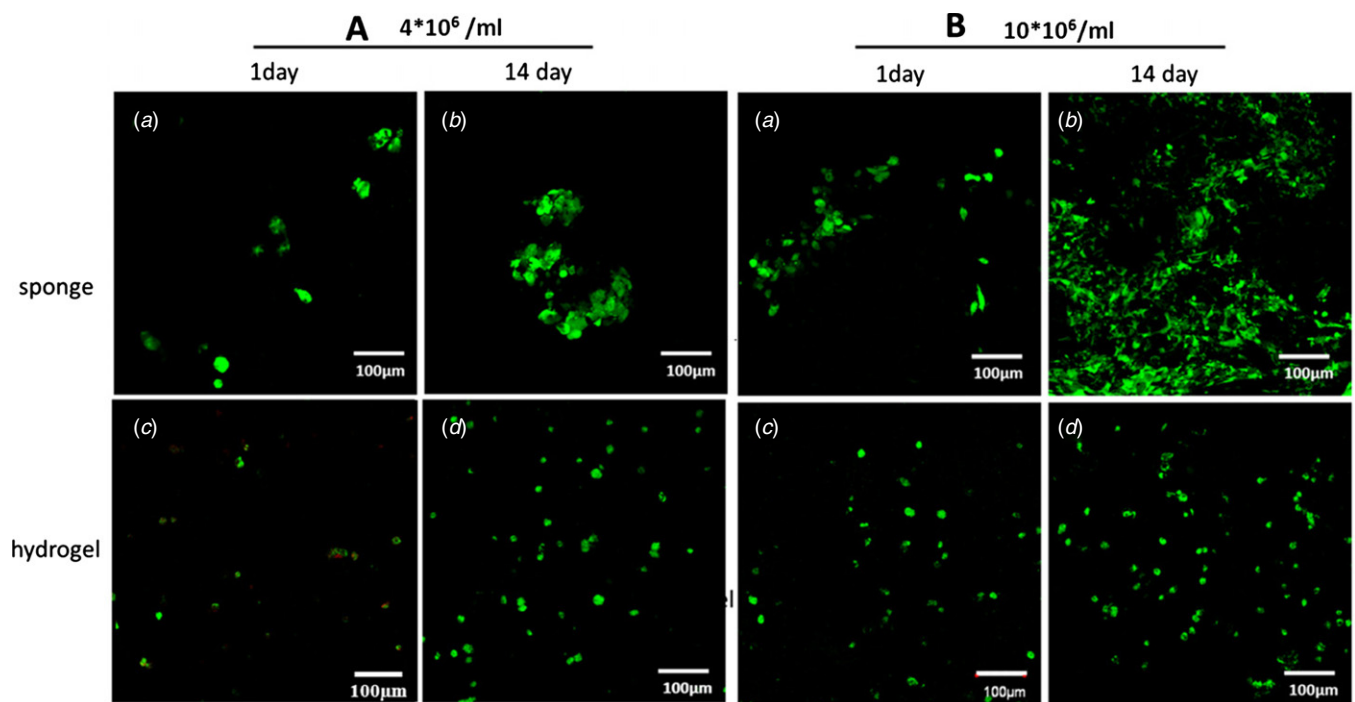


**Figure 3.** MSCs viability in scaffolds stained with FDA-PI staining. (A) MSCs with cell density  $4 \times 10^6 \text{ ml}^{-1}$  in sponges (a), (b) and in hydrogels (c), (d) at day 1 and day 14; (B) MSCs with cell density of  $10 \times 10^6/\text{ml}$  in sponges (a), (b) at day 1 and day 14 and in hydrogels (c), (d) at day 1 and day 14. Live cells were stained by FDA (green) and dead cells were stained by PI (red). Scale bars:  $100 \mu\text{m}$ .

lower cell density formed little clusters at day 1 and developed into larger colonies of cell aggregates at day 14 (figure 3). Compared with the low cell density group, more extensive cell aggregation appeared in the sponge at day 1 with the high cell density seeding, and widespread distribution of the cell aggregation was detected by day 14. MSCs in the hydrogels were distributed evenly, but without cell–cell contact. The number of cells remained nearly unchanged with time and minimal cell–cell contact was observed at day 14 even in the high cell density sample.

MSC morphology within the two systems was further examined by phalloidin staining of F-actin (figures 4 and 5). Cell aggregation with extensive stress fibers was observed at seven days in the sponge. More extensive cell–cell interaction appeared in the sponge with higher cell seeding (figure 5) compared to the lower cell concentration group (figure 4). As for the hydrogel, MSCs scattered homogeneously, maintained round morphology even with high cell density seeding. Lack of cell–cell communication remained unchanged during the seven day period.

### 3.3. DNA and sGAG analysis

Quantification of DNA at 21 days after chondrogenic differentiation showed significantly higher amount of DNA in the sponge than in hydrogel both in low cell density ( $p = 0.031$ ) and high cell density group ( $p < 0.01$ ) (figure 6). Significantly higher DNA content was found in the constructs with high cell density than that of the low density group both in the sponge ( $p < 0.01$ ) and in the hydrogel ( $p = 0.013$ ). Compared with MSCs in the hydrogel, MSCs in the sponge constructs deposited significantly higher sGAG ( $p < 0.01$ )

in the high density group by 21 days. In sponges, the high cell density group secreted more sGAG content than the low density group ( $p < 0.01$ ). Slightly higher amount of sGAG was observed in the higher cell density hydrogel sample than the lower cell density samples, although these differences were not significant ( $p = 0.137$ ). GAG content normalized to DNA showed that there was no significant difference between the different cell densities or between the sponge and hydrogel.

### 3.4. Histology and immunohistochemistry

Immunohistochemical staining for GAG, collagen II and collagen X with cell concentration at  $10 \times 10^6 \text{ cells ml}^{-1}$ , showed intense staining in sponge constructs at day 21, whereas there was nearly no staining in the hydrogel (figures 7 and 8). As for collagen I, there was only isolated staining associated with cells in the hydrogel compared with the extensive staining in the sponge (figure 8).

## 4. Discussion

Cells can recognize microenvironment factors and adapt their behaviour to these factors, resulting in changes in phenotype maintenance, cytoskeleton spreading, proliferation, gene expression and ECM secretion through metabolic activity, cell–matrix and cell–cell contact (Kumar *et al* 2011, Mao *et al* 2012). In our previous study, *in vitro* chondrogenic outcome of expanded chondrocytes was comparable between the sponge and hydrogel though initial behaviour was different due to the complex physical environment factors involved (Zhang *et al* 2013). In this study, we extended the research to bone marrow-derived MSCs. MSCs in the

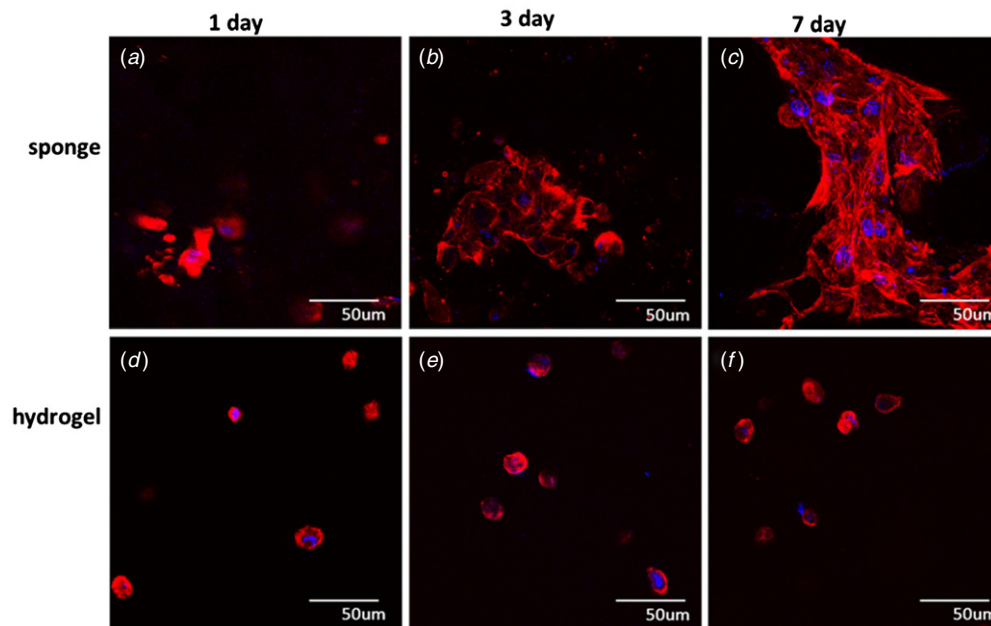


**Figure 4.** F-actin staining of MSCs with cell density  $4 \times 10^6 \text{ ml}^{-1}$ . MSCs in sponges (a), (b), (c) and hydrogels (d), (e), (f) at 1, 3 and 7 days. F-actin was stained red while the cell nucleus was blue. Scale bars:  $50 \mu\text{m}$ .

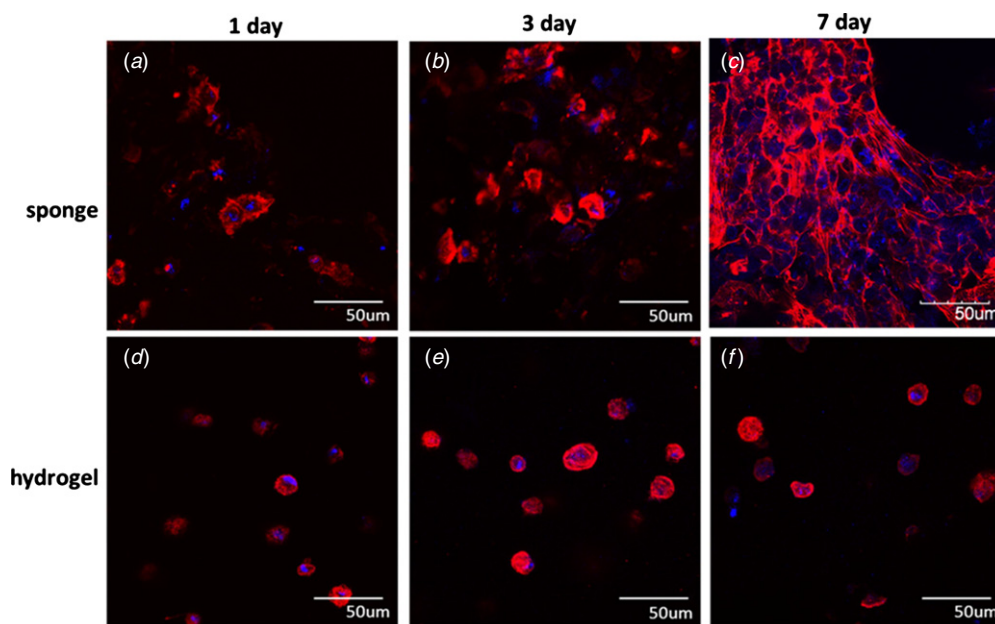


**Figure 5.** F-actin staining of MSCs with cell density of  $10 \times 10^6 \text{ ml}^{-1}$  within sponges (a), (b), (c) and hydrogels (d), (e), (f) at 1, 3 and 7 days. F-actin was stained red while the cell nucleus was blue. Scale bars:  $50 \mu\text{m}$ .

sponge proliferated rapidly and underwent more efficient chondrogenic differentiation indicated by the expression of sGAG, collagen type I, II and X. Notably, there was little proliferation and lack of cartilage tissue formation in the hydrogel with increased seeding density. The different tissue forming ability in these two scaffolds could be attributed to the special metabolic requirement of MSCs and the particular cellular events prerequisite in the differentiation process of MSCs. However, when normalized against the DNA content, the sGAG deposition per DNA unit was no different between sponge and hydrogel, suggesting that MSC in the sponges and

hydrogels underwent chondrogenic differentiation to similar extents, and that the overall significantly better cartilage matrix formation in the sponges was due to more cells. MTT assay at early time points and DNA quantification after differentiation both indicated higher cell proliferation in the sponge while cells in the hydrogel remained relatively inert. It was shown in our previous study that due to smaller pore size and low structural interconnectivity of the hydrogel compared to the sponge, cells within the two systems are subjected to disparate levels of nutrients and chondrogenic induction factors, with the hydrogel having limited nutrient diffusion (Zhang *et al* 2013).

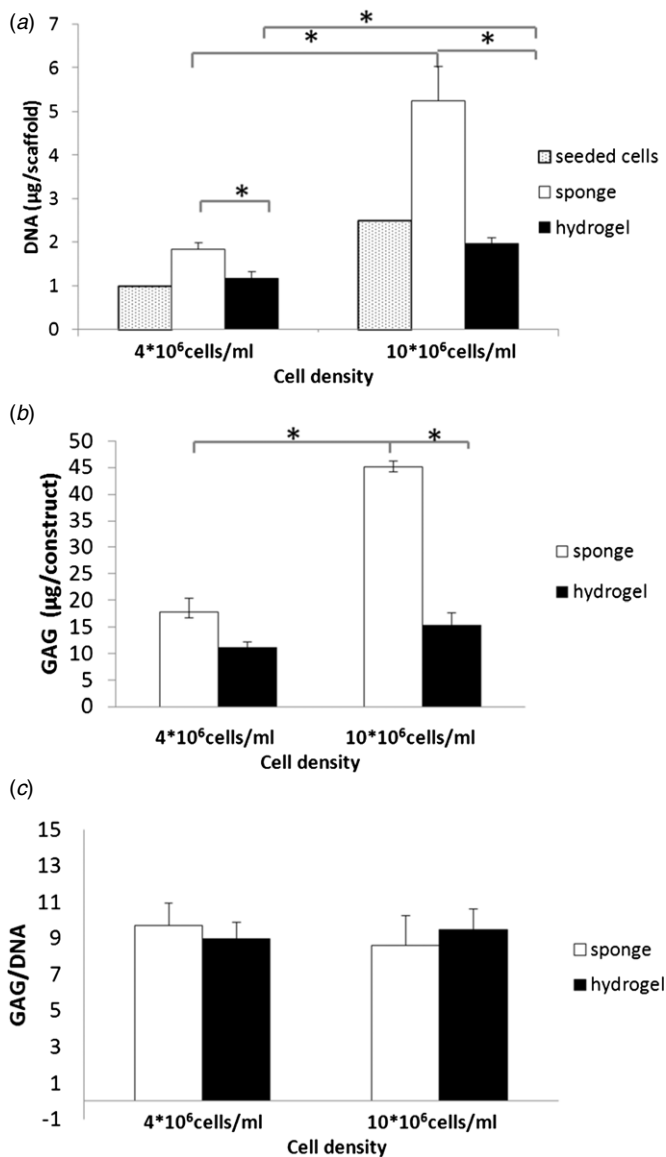


**Figure 6.** Quantification of chondrogenic differentiation of MSCs in sponges and hydrogels with cell density of  $4 \times 10^6$  ml<sup>-1</sup> and  $10 \times 10^6$  ml<sup>-1</sup> after three weeks differentiation. Total DNA (a) and sGAG (b) were quantified in the scaffold constructs. GAG was normalized to the DNA at three weeks (c). Data expressed as mean  $\pm$  SD ( $n = 3$ ) \* represents  $p < 0.05$ . (The standard deviation was used to define the value of the error bars.)

While the inert niche in the hydrogel might be preferred by chondrocytes, a cell type conditioned to function in constrained and nutrient poor avascular environment of the native cartilage tissue (Mobasher *et al* 2005), MSCs, lack the ability to function in a constrained environment and can only function anabolically in regions with ample nutrient supply (Farrell *et al* 2012). The low diffusive environment of hydrogel could be a contributing factor that resulted in metabolic inactivity and lack of proliferation of MSCs in this scaffold.

Elastic modulus of the sponges (195.3 kPa) was significant higher than that of the hydrogels (2.0 kPa), as reported in our previous study (Zhanget *al* 2013). Increasing matrix stiffness disrupts cell morphology, and leads to increased proliferation. Stiffer substrate was demonstrated to promote

the proliferation of chondrocytes (Schuh *et al* 2010) mammary epithelia (Paszek *et al* 2005) and glioma cells (Ulrich *et al* 2009). In this study, the higher proliferation of MSCs in the sponge may be partly due to the stiffness of the sponge. In addition, a suitable Young's Modulus (0.4–0.8 MPa) (Little *et al* 2011, Moutos *et al* 2007) is particularly important for neo-cartilage development and the Young's modulus of the sponge (195.3 kPa) was much closer to 0.4 MPa than that of the hydrogel (2.0 kPa). MSCs were demonstrated to differentiate to specify lineage and commit to phenotypes with extreme sensitivity to tissue level elasticity (Engler *et al* 2006). For example, soft matrices that mimic brain are neurogenic and rigid matrices that mimic bone prove osteogenic. Thus, the sponge with the Young's modulus close to native cartilage may also be more conducive for the MSC chondrogenic differentiation.

Conversely, the different tissue formation ability in these two scaffolds could also be attributed to the particular cellular events prerequisite in the chondrogenic differentiation process of MSCs. The distinctly different morphology of the MSCs in these two scaffolds might make a direct impact on subsequent differentiation. Chondrogenesis of MSCs is associated with morphologic changes from fibroblast to spherical morphology, in which the fibroblastic morphology is formed through cell–matrix interactions during migration and proliferation, and develops into spherical morphology in the process of condensation (DeLise *et al* 2000). The chondrogenic differentiation of MSCs occurs in tightly-orchestrated stages. Aggregation of mesenchymal cells into precartilage condensations is crucial for chondrogenesis. Condensation occurs through cell–cell contacts, which is regulated by the association of cell adhesion molecules of the adjacent cells, formation of gap junctions and changes in the cytoskeletal architecture, subsequently activating intracellular signalling pathways to initiate the transition from chondroprogenitor cells to a fully committed chondrocyte (DeLise *et al* 2000, Goldring *et al* 2006, Raghothaman *et al* 2014). The ability of MSCs to aggregate in the larger pores in the sponge scaffold, coupled with proliferation of cells within the sponge, could have facilitated chondrogenic condensation process of MSCs. In contrast, MSCs within the hydrogel remained as single cells, even with higher seeding density. The lack of contact among the encapsulated cells in hydrogel could have directly hindered their chondrogenic differentiation.

It is worth noting that in studies evaluating the quality of cartilage matrix generated by chondrocytes versus MSCs-derived cartilage in which hydrogel scaffold was employed, researchers invariably found that the MSCs-derived constructs were both biochemically and mechanically inferior compared to chondrocytes-based construct (Erickson *et al* 2009, Huang *et al* 2008, 2010), even with higher seeding density of MSCs up to  $60 \times 10^6$  cells ml<sup>-1</sup> (Huang *et al* 2009). Compared to the lack of MSCs' chondrogenic differentiation detected in our chitosan hydrogel system, apart from the accessibility of nutrient diffusion, the relatively low seeding cell density adopted in our study might also be a contributing factor. Increasing cell seeding density in hydrogel was indeed found to improve the quality of cartilage construct from

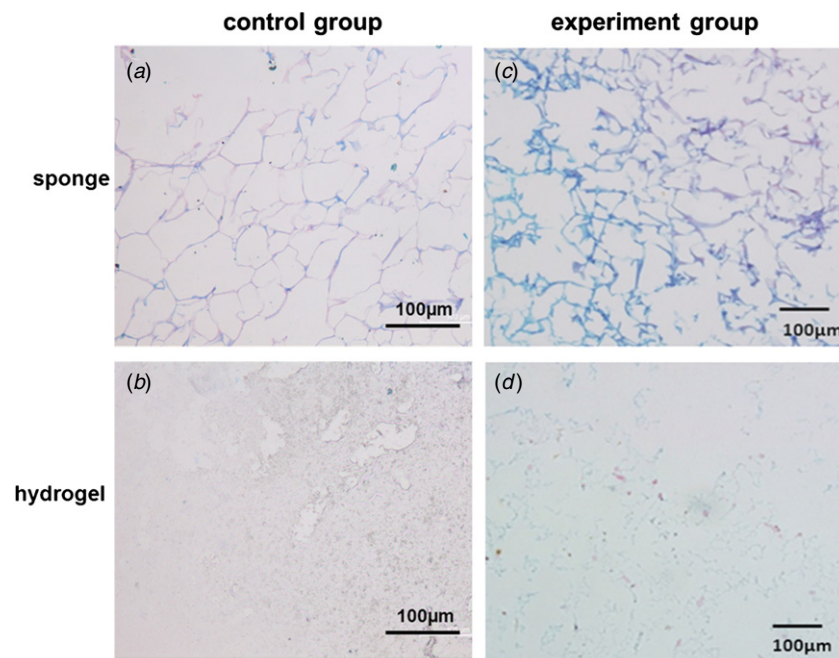


**Figure 7.** Alcian blue staining of cell-scaffold constructs after three weeks *in vitro* differentiation. Blank sponge (a), experiment sponge (c), blank hydrogel (b) and experiment hydrogel (d). Scale bars: 100  $\mu\text{m}$ .

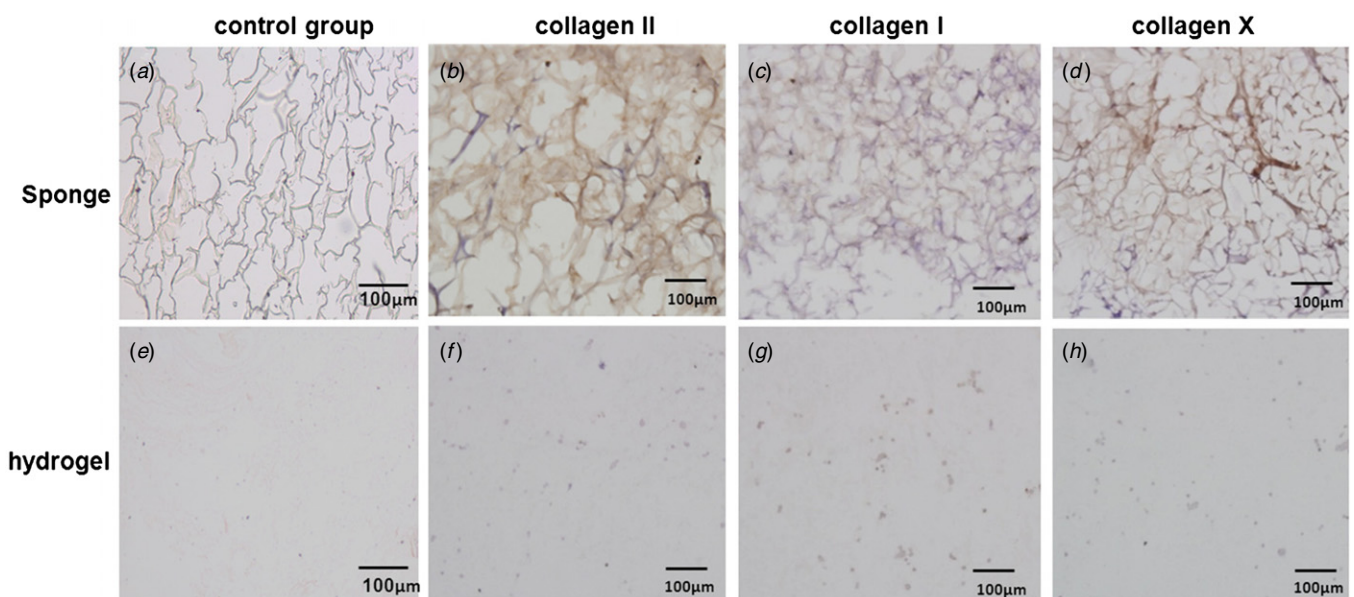


**Figure 8.** Immunohistochemical staining of collagen I, II and X in cell-scaffold constructs after three weeks *in vitro* differentiation. Immunohistochemical staining of blank sponge (a) and blank hydrogel (e); collagen type II staining of sponge (b) and hydrogel (f); collagen type I staining of sponge (c) and hydrogel (g); collagen type X staining of sponge (d) and hydrogel (h). Scale bars: 100  $\mu\text{m}$ .

MSCs (Erickson *et al* 2012, Huang *et al* 2008). This was, however, limited to the hydrogel with lower cross-linking that might facilitate cell–cell contact and higher nutrient diffusion (Bian *et al* 2013b). Of note, many hydrogels inherently limit the direct cell–cell interactions. Among the hydrogels tested, both agarose and hyaluronic acid hydrogel maintained MSCs with limited cell–cell interaction (unless seeded at very high concentration). Chondrogenic outcome of MSCs in the two above mentioned hydrogels was lower compared to cells in the self-assembling peptide

hydrogel for which MSCs adopted a fibroblastic morphology with the appearance of cell–cell contact (Erickson *et al* 2009). The importance of cell–cell interaction in MSCs-based cartilage tissue development was further demonstrated by the functionalization of a hyaluronic acid hydrogel with conjugation of N-cadherin mimetic peptides, (Bian *et al* 2013a) and the proximal interactions between MSCs and the extracellular matrix that promote extensive cell–cell interaction through membranous N-cadherin expression (Raghothaman *et al* 2014). N-cadherin, a key factor in directing

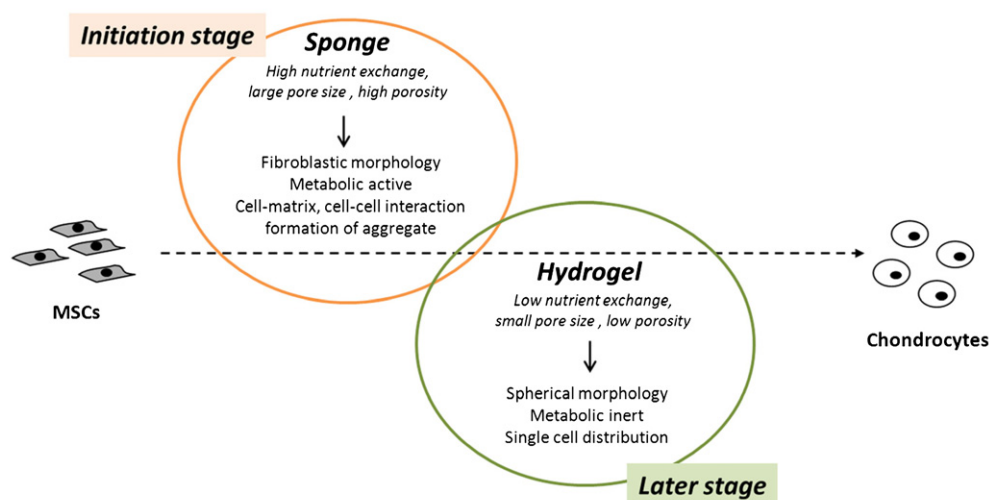


**Figure 9.** Schematic diagram outlining cellular requirement for MSCs and chondrocytes during chondrogenic differentiation provided by sponge and hydrogel scaffolds, respectively.

cell–cell interactions during mesenchymal condensation, promoted both early chondrogenesis of MSCs and cartilage-specific matrix production within the hydrogel construct.

In this study, we found that the hydrogel provided a relatively inert niche and encapsulated cells lacked nutrition exchange and cell–cell contact. Degradable, bioactive, composite hydrogels are a possible solution to overcome this challenge. Cell-degradable hydrogels, such as matrix metalloproteinase degradable hydrogels were created to facilitate the condensation process of MSCs and found to increase levels of specific differentiation markers compared to non-degradable hydrogels group (Anderson *et al* 2011). Han *et al* (2013) successfully created 3D hydrogels with dynamically tunable macro-porosity. In this hydrogel, cell proliferation and extracellular matrix production were markedly enhanced by sequential desorption of the embedded macrospores with exposure to specific stimuli at various time points. Bioactive hydrogels were fabricated by modifying hydrogel with several amino acid sequences including RGD (Salinas and Anseth 2008), IKLLI, GFOGERGD (Mhanna *et al* 2014) sequence or large molecules such as collagen. This allowed MSCs to crosstalk with the microenvironment. To solve the cell–cell contact challenge, implantation of micro-aggregations of MSCs rather than single cell solution into hydrogels, was adopted to significantly accelerate hyaline cartilage formation was observed (Hayashi and Tabata 2011). Rather than increasing crosslink density that will impair the diffusion of nutrients (Bryant 2004), composite scaffolds were fabricated such as filling the hydrogel into the sponge (Wang *et al* 2010) or mixing nanofibers or microspheres into hydrogel to enhance the mechanical properties.

Taken together, when analysing the different tissue formation ability of chondrocytes and MSCs in hydrogel, our results suggest that MSCs and chondrocyte, possessing different metabolic requirements and developmental status,

will require differing physical microenvironments for cartilage tissue formation (figure 9). The drastically different tissue formation ability between MSCs and chondrocytes in hydrogel and sponge highlight the requirement for specific scaffold designs catering to specific cell types in cartilage tissue engineering. In the chondrogenic differentiation process of MSCs to chondrocytes, engineering scaffolds with the ability to transit from the form of sponge to hydrogel might be desirable for cartilage regeneration.

## 5. Conclusion

MSCs distribution, morphology and proliferation differed in the sponge and hydrogel, which affected cartilage formation in the two scaffold systems. MSCs were able to undergo robust chondrogenic differentiation in the sponge due to their ability to proliferate efficiently and form cell aggregates, which are essential for the initiation of chondrogenic differentiation. In contrast, the overall tissue formation ability of MSCs in the hydrogel was hindered by the low proliferation and the lack of cell–cell interaction though both cells in sponges and hydrogels undergo chondrogenic differentiation to a similar extent. The drastically different tissue formation ability of MSCs in hydrogel and sponge highlight the requirement for specific design of scaffold for the chondrogenic differentiation of MSCs in cartilage tissue engineering.

## Acknowledgments

The authors acknowledge support from the National Basic Research Program of China grant (973 Program) (2012CB619100), as well as the National Natural Science Foundation of China grant (81271722). The major part of this project was performed in National University of Singapore, Tissue Engineering Program.

## References

- Anderson S B, Lin C C, Kuntzler D V and Anseth K S 2011 The performance of human mesenchymal stem cells encapsulated in cell-degradable polymer-peptide hydrogels *Biomaterials* **32** 3564–74
- Bian L, Guvendiren M, Mauck R L and Burdick J A 2013a Hydrogels that mimic developmentally relevant matrix and N-cadherin interactions enhance MSC chondrogenesis *Proc. Natl Acad. Sci. USA* **110** 10117–22
- Bian L, Hou C, Tous E, Rai R, Mauck R L and Burdick J A 2013b The influence of hyaluronic acid hydrogel crosslinking density and macromolecular diffusivity on human MSC chondrogenesis and hypertrophy *Biomaterials* **34** 413–21
- Bryant S J, Chowdhury T T, Lee D A, Bader D L and Anseth K S 2004 Crosslinking density influences chondrocyte metabolism in dynamically loaded photocrosslinked PEG hydrogels *Ann. Biomed. Eng.* **32** 407–17
- Caplan A I 2005 Mesenchymal stem cells: cell-based reconstructive therapy in orthopedics *Tissue Eng.* **11** 1198–211
- Choi S W, Yeh Y C, Zhang Y, Sung H W and Xia Y N 2010 Uniform beads with controllable pore sizes for biomedical applications *Small* **6** 1492–8
- DeLise A M, Fischer L and Tuan R S 2000 Cellular interactions and signaling in cartilage development *Osteoarthritis Cartilage* **8** 309–34
- Engler A J, Sen S, Sweeney H L and Discher D E 2006 Matrix elasticity directs stem cell lineage specification *Cell* **126** 677–89
- Erickson I E, Huang A H, Chung C, Li R T, Burdick J A and Mauck R L 2009 Differential maturation and structure–function relationships in mesenchymal stem cell and chondrocyte-seeded hydrogels *Tissue Eng. A* **15** 1041–52
- Erickson I E, Kestle S R, Zellars K H, Farrell M J, Kim M, Burdick J A and Mauck R L 2012 High mesenchymal stem cell seeding densities in hyaluronic acid hydrogels produce engineered cartilage with native tissue properties *Acta Biomater.* **8** 3027–34
- Farrell M J, Comeau E S and Mauck R L 2012 Mesenchymal stem cells produce functional cartilage matrix in three-dimensional culture in regions of optimal nutrient supply *Eur. Cells Mater.* **23** 425–40 (PMID: 22684531)
- Ge Z, Li C, Heng B C, Cao G and Yang Z 2012 Functional biomaterials for cartilage regeneration *J. Biomed. Mater. Res. A* **100** 2526–36
- Goldring M B, Tsuchimochi K and Ijiri K 2006 The control of chondrogenesis *J. Cell. Biochem.* **97** 33–44
- Han L H, Lai J H, Yu S and Yang F 2013 Dynamic tissue engineering scaffolds with stimuli-responsive macroporosity formation *Biomaterials* **34** 4251–8
- Hao T, Wen N, Cao J K, Wang H B, Lu S H, Liu T, Lin Q X, Duan C M and Wang C Y 2010 The support of matrix accumulation and the promotion of sheep articular cartilage defects repair *in vivo* by chitosan hydrogels *Osteoarthritis Cartilage* **18** 257–65
- Hayashi K and Tabata Y 2011 Preparation of stem cell aggregates with gelatin microspheres to enhance biological functions *Acta Biomater.* **7** 2797–803
- Hoemann C D, Sun J, Legare A, McKee M D and Buschmann M D 2005 Tissue engineering of cartilage using an injectable and adhesive chitosan-based cell-delivery vehicle *Osteoarthritis Cartilage* **13** 318–29
- Huang A H, Stein A and Mauck R L 2010 Evaluation of the complex transcriptional topography of mesenchymal stem cell chondrogenesis for cartilage tissue engineering *Tissue Eng. A* **16** 2699–708
- Huang A H, Stein A, Tuan R S and Mauck R L 2009 Transient exposure to transforming growth factor beta 3 improves the mechanical properties of mesenchymal stem cell–laden cartilage constructs in a density-dependent manner *Tissue Eng. A* **15** 3461–72
- Huang A H, Yeger-McKeever M, Stein A and Mauck R L 2008 Tensile properties of engineered cartilage formed from chondrocyte- and MSC-laden hydrogels *Osteoarthritis Cartilage* **16** 1074–82
- Kang N *et al* 2012 Effects of co-culturing BMSCs and auricular chondrocytes on the elastic modulus and hypertrophy of tissue engineered cartilage *Biomaterials* **33** 4535–44
- Kumar G, Tison C K, Chatterjee K, Pine P S, McDaniel J H, Salit M L, Young M F and Simon C G 2011 The determination of stem cell fate by 3D scaffold structures through the control of cell shape *Biomaterials* **32** 9188–96
- Little C J, Bawolin N K and Chen X 2011 Mechanical properties of natural cartilage and tissue-engineered constructs *Tissue Eng. B Rev.* **17** 213–27
- Li W J, Jiang Y J and Tuan R S 2006 Chondrocyte phenotype in engineered fibrous matrix is regulated by fiber size *Tissue Eng.* **12** 1775–85
- Mao M, He J, Liu Y, Li X and Li D 2012 Ice-template-induced silk fibroin-chitosan scaffolds with predefined microfluidic channels and fully porous structures *Acta Biomater.* **8** 2175–84
- Mhanna R, Ozturk E, Vallmajo-Martin Q, Millan C, Muller M and Zenobi-Wong M 2014 GFOGER-modified MMP-sensitive polyethylene glycol hydrogels induce chondrogenic differentiation of human mesenchymal stem cells *Tissue Eng. A* **20** 1165–74
- Mobasheri A, Richardson S, Mobasheri R, Shakibaei M and Hoyland J A 2005 Hypoxia inducible factor-1 and facilitative glucose transporters GLUT1 and GLUT3: Putative molecular components of the oxygen and glucose sensing apparatus in articular chondrocytes *Histol. Histopathol.* **20** 1327–38 (PMID: 16136514)
- Moutos F T, Freed L E and Guilak F 2007 A biomimetic three-dimensional woven composite scaffold for functional tissue engineering of cartilage *Nature Mater.* **6** 162–7
- Nuernberger S, Cyran N, Albrecht C, Redl H, Vecsei V and Marlovits S 2011 The influence of scaffold architecture on chondrocyte distribution and behavior in matrix-associated chondrocyte transplantation grafts *Biomaterials* **32** 1032–40
- Paszek M J *et al* 2005 Tensional homeostasis and the malignant phenotype *Cancer Cell* **8** 241–54
- Qi Y, Feng G and Yan W 2012 Mesenchymal stem cell-based treatment for cartilage defects in osteoarthritis *Mol. Biol. Rep.* **39** 5683–9
- Qing C, Wei-ding C and Wei-min F 2011 Co-culture of chondrocytes and bone marrow mesenchymal stem cells *in vitro* enhances the expression of cartilaginous extracellular matrix components *Brazilian J. Med. Biol. Res.* **44** 303–10
- Raghothaman D, Leong M F, Lim T C, Toh J K, Wan A C, Yang Z and Lee E H 2014 Engineering cell matrix interactions in assembled polyelectrolyte fiber hydrogels for mesenchymal stem cell chondrogenesis *Biomaterials* **35** 2607–16
- Saha S, Kirkham J, Wood D, Curran S and Yang X 2010 Comparative study of the chondrogenic potential of human bone marrow stromal cells, neonatal chondrocytes and adult chondrocytes *Biochem. Biophys. Res. Commun.* **401** 333–8
- Salinas C N and Anseth K S 2008 The enhancement of chondrogenic differentiation of human mesenchymal stem cells by enzymatically regulated RGD functionalities *Biomaterials* **29** 2370–7
- Schuh E, Kramer J, Rohwedel J, Notbohm H, Muller R, Gutschmann T and Rotter N 2010 Effect of matrix elasticity on the maintenance of the chondrogenic phenotype *Tissue Eng.* **16** 1281–90
- Ulrich T A, de Juan Pardo E M and Kumar S 2009 The mechanical rigidity of the extracellular matrix regulates the structure, motility, and proliferation of glioma cells *Cancer Res.* **69** 4167–74

- Vinardell T, Buckley C T, Thorpe S D and Kelly D J 2011 Composition-function relations of cartilaginous tissues engineered from chondrocytes and mesenchymal stem cells isolated from bone marrow and infrapatellar fat pad *J. Tissue Eng. Regenerative Med.* **5** 673–83
- Wang C-C, Yang K-C, Lin K-H, Liu H-C and Lin F-H 2011 A highly organized three-dimensional alginate scaffold for cartilage tissue engineering prepared by microfluidic technology *Biomaterials* **32** 7118–26
- Wang W, Li B, Li Y L, Jiang Y Z, Ouyang H W and Gao C Y 2010 *In vivo* restoration of full-thickness cartilage defects by poly(lactide-co-glycolide) sponges filled with fibrin gel, bone marrow mesenchymal stem cells and DNA complexes *Biomaterials* **31** 5953–65
- Woods A, Weng G Y and Beier Y 2007 Regulation of chondrocyte differentiation by the actin cytoskeleton and adhesive interactions *J. Cell. Biophysiol.* **213** 1–8
- Wu X, Liu Y, Li X, Wen P, Zhang Y, Long Y, Wang X, Guo Y, Xing F and Gao J 2010 Preparation of aligned porous gelatin scaffolds by unidirectional freeze-drying method *Acta Biomater.* **6** 1167–77
- Yang Z, Wu Y N, Li C, Zhang T T, Zou Y, Hui J H P, Ge Z G and Lee E H 2012 Improved mesenchymal stem cells attachment and *in vitro* cartilage tissue formation on chitosan-modified poly(l-lactide-co-epsilon-caprolactone) scaffold *Tissue Eng. A* **18** 242–51
- Zanetti N C and Solursh M 1984 Induction of chondrogenesis in limb mesenchymal cultures by disruption of the actin cytoskeleton *J. Cell Biol.* **99** 115–23
- Zhang J J, Yang Z, Li C, Dou Y, Li Y J, Thote T, Wang D and Ge Z G 2013 Cells behave distinctly within sponges and hydrogels due to differences of internal structure *Tissue Eng. A* **19** 2166–75